2021 43rd Annual International Conference of the
IEEE Engineering in Medicine & Biology Society (EMBC)
Oct 31 - Nov 4, 2021. Virtual Conference

A Quarter-split Domain-adaptive Network for EGFR Gene Mutation Prediction in Lung Cancer by Standardizing Heterogeneous CT image

Liusu Wang[1], Shuo Wang[1], He Yu[2], Yongbei Zhu[1], Weimin Li[2], and Jie Tian[1], *IEEE Fellow*

***Abstract*— Epidermal growth factor receptor (EGFR) gene mutation status is crucial for the treatment planning of lung cancer. The gold standard for detecting EGFR mutation status relies on invasive tumor biopsy and expensive gene sequencing. Recently, computed tomography (CT) images and deep learning have shown promising results in non-invasively predicting EGFR mutation in lung cancer. However, CT scanning parameters such as slice thickness vary largely between different scanners and centers, making the deep learning models very sensitive to noise and therefore not robust in clinical practice. In this study, we propose a novel $QuarterNet_{adaptive}$ model to predict EGFR mutation in lung cancer, which is robust to CT images of different thicknesses. We propose two components: 1) a quarter-split network to sequentially learn local lung features from different lung lobes and global lung features; 2) a domain adaptive strategy to learn CT thickness-invariant features. Furthermore, we collected a large dataset including 1413 patients with both EGFR gene sequencing and CT images of various thicknesses to evaluate the performance of the proposed model. Finally, the $QuarterNet_{adaptive}$ model achieved AUC over 0.88 regarding CT images of different thicknesses, which improves largely than state-of-the-art methods.**

***Clinical relevance*— We proposed a non-invasive model to detect EGFR gene mutation in lung cancer, which is robust to CT images of different thicknesses and can assist lung cancer treatment planning.**

I. INTRODUCTION

Epidermal growth factor receptor (EGFR) gene mutation status is critical for the treatment planning of lung cancer. According to the NCCN guideline, EGFR-targeted therapy is the first-line treatment for EGFR-mutant patients, while other treatments (e.g., chemotherapy) are recommended for EGFR-wild type patients [1]. Currently, EGFR mutation status is determined by invasive tumor tissue biopsy and expensive gene sequencing. Therefore, non-invasive and low-cost manners are in need. Computed tomography (CT), as a routinely used technique in lung cancer analysis, is non-invasive, cost-effective, and enables us to observe the whole tumor instead of a small part of tumor tissues.

Liusu Wang and Shuo Wang contribute equally. Weimin Li (weimi003@scu.edu) and Jie Tian (tian@ieee.org) are co-corresponding authors.

[1]is with the Beijing Advanced Innovation Center for Big Data-based Precision Medicine, School of Medicine, Beihang University, Beijing, China; CAS Key Laboratory of Molecular Imaging, Institute of Automation, Chinese Academy of Sciences, Beijing, China. [2]is with the Department of Critical Care and Respiratory Medicine, West China Hospital of Sichuan University, Chengdu, China.

This work was supported in part by the National Natural Science Foundation of China (82001913, 81930053, 62027901), and China Postdoctoral Science Foundation (2019TQ0019, 2020M670101)

Recently, deep learning has shown promising results in predicting EGFR mutation status and many clinical outcomes using CT images [2]. However, CT images are heterogeneous between different scanners and centers, which affects deep learning models largely. For instance, CT slice thickness can cause data distribution gaps and finally affects model performance [3], [4]. As shown in Fig. 1a and Fig. 1b, thin-slice CT image (slice thickness $\leq$ 2mm) provides more detailed texture information but introduces more noise. On the contrary, thick-slice CT image (slice thickness $\geq$ 3mm) includes less noise but losses detailed texture information (Fig. 1c and Fig. 1d). CT images from different scanners and centers usually have many different slice thicknesses, which makes deep learning models only applicable to a limited dataset in many situations. Therefore, methods that can be adaptive to CT images of different thicknesses are necessary [4].

Recent studies have shown that image pre-processing methods such as re-sample, compensatory transformation, and gray level normalization are feasible to reduce scanning parameter effects of CT image [5], [6]. However, due to the data-driven manner and strong feature learning ability, deep learning models can easily learn subtle noise from different image parameters (e.g., texture variance caused by different slice thickness in CT) [7]. How to force the model to focus on learning task-related pathological features and decrease the data distribution gaps caused by different scanning parameters in medical images attracts many recent studies. Recently, domain adaption methods have shown promising results in dealing with images acquired from different equipment or tasks [8], [9]. In domain adaption methods, images with large differences can be treated as from different domains. Afterward, a Siamese network that simultaneously inputs image pairs from different domains is used, forcing the dual network to learn features that are robust and transferable between different domains.

This study presents a deep domain adaptive model to solve the data distribution gap caused by image slice thickness, making the deep learning model adaptive to CT images of different slice thicknesses. We propose a quarter-split network to learn features from different lung lobes simultaneously, aiming at extracting structural information from different lung regions that can probably reflect EGFR gene mutation status in lung cancer. Meanwhile, a Siamese network architecture is built to learn features that are robust to images of different slice thicknesses.

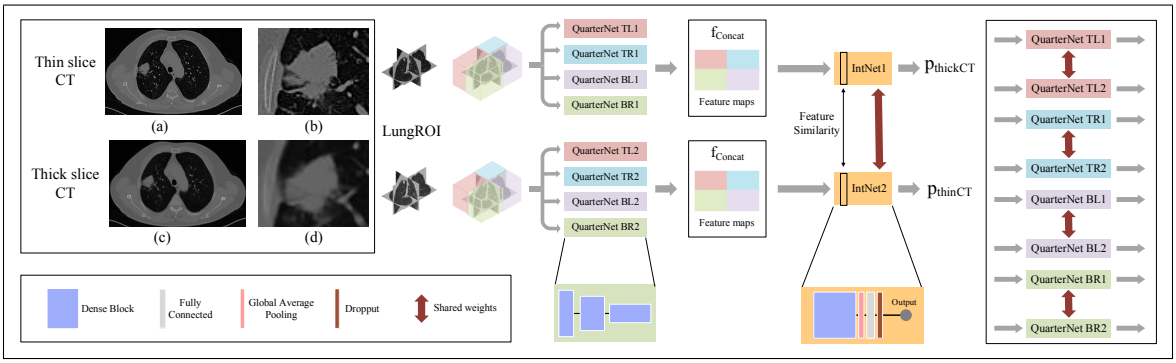

Fig. 1. The left part depicts CT images with different slice thicknesses. (a) and (b) are the thick CT image (thickness=5mm) and the cropped tumor region; (c) and (d) are thin CT images (thickness=1mm) and the cropped tumor region. a) and c) are from the same patient. The right part of this figure depicts the framework of the proposed $QuarterNet_{adaptive}$ model. This model includes two CNN branches with shared weights and accepts paired images as input. Each branch consists of four quarter-split networks (QuarterNets) and an integrated network (IntNet). The four QuarterNets are independent in the same branch but share weights between the two branches.

II. METHODS

As illustrated in Fig. 1, the proposed model consists of two weight-shared convolutional neural network (CNN) branches to deal with images from different domains. Here, we treat thin-slice images and thick-slice images as two image domains and input them to the two CNN branches respectively. In each branch, we first propose a quarter-split network to learn local features focusing on different lung regions, and then concatenate the sub-region feature maps to learn global lung features.

A. Quarter-split network to learn local and global lung features

Inspired by a recent study that disease information can be reflected in the whole lung [10], we adopt a whole lung analysis manner to extract comprehensive information including both tumor area and the whole lung area for EGFR gene mutation prediction. We first use a DenseNet-FPN model to segment lung area in CT image automatically [10] and use the 3D bounding box of the segmented area as regions of interest (lung-ROI). Second, the lung-ROI is resized into 48×240×360 voxels and standardized into $0-mean$ and $1-std$ intensities through z-score normalization for further analysis. Different from previous studies, we propose a quarter-split network (QuarterNet) to extract local lung features from four lung regions. As shown in Fig. 1, each lung-ROI is uniformly split into four sub-regions on the axial plane (TL1, TR1, BL2, BR2). For example, the i_{th} input image X^i is split according to:

$$X^i = \begin{pmatrix} X^i_{tl} & X^i_{tr} \\ X^i_{bl} & X^i_{br} \end{pmatrix} = \sum_{m,n=1}^{2} X^i_{m,n} \tag{1a}$$

$$\text{where} \quad X^i_{1,1} = \begin{pmatrix} X^i_{tl} & O \\ O & O \end{pmatrix}, \text{etc} \tag{1b}$$

where X_{tl}, X_{tr}, X_{bl}, X_{br} indicate the top-left, top-right, bottom-left, bottom-right sub-region of the lung, respectively. Here, the QuarterNet is the same as the first three dense blocks of the COVID19-Net in a recently published study [10], which has been proved effective in analyzing lung CT images.

Afterward, the four sub-regions are fed into the corresponding quarter encoders $E_{quarter,m,n}$ for local lung feature extraction, which enables the model to learn specific features of different lung lobes. Then, we concatenate the four feature maps from the QuarterNets, aiming at mapping the detailed local lung features into the whole lung space. Finally, we build an IntNet (E_{int}) to learn global lung features for the EGFR gene mutation prediction. The IntNet uses a similar structure with the last dense block of the previous COVID19-Net with few modifications. After the global average pooling layer of the last dense block, we use a fully connected layer (64 units), a dropout layer, and the final output layer with a sigmoid activation function. Given the i_{th} input image X^i, the predicted EGFR mutation probability pi is:

$$p^i = E\left(I^i\right) = E_{int}\left(\sum_{m,n=1}^{2} E_{quart,m,n}\left(X^i_{m,n}\right)\right) \tag{2}$$

B. Domain adaption strategy to learn robust features invariant to CT thickness

The domain adaptation strategy uses a Siamese-net architecture to learn the CT thickness-invariant features from two paired images from different domains. The network includes two branches (thin-CT branch and thick-CT branch) sharing the same architecture. During training, We input image pairs from the two domains (thin-CT domain and thick-CT domain) to the two CNN branches, respectively. Each image pair includes a thin CT image and a thick CT image from the same patient. To enable the network to learn thickness-invariant features, we use feature similarity loss (L_s) after the fully connected layer in the IntNet, which forces the network to extract local and global lung features that are invariant in images of different CT thicknesses, aiming at shrinking the data distribution gap of the two domains.

$$L_s = \sum_i \left\| f^{thin}\left(X^i_{thinCT}\right) - f^{thick}\left(X^i_{thickCT}\right)\right\|_2 \tag{4}$$

TABLE I

RESULTS OF THE MODELS THAT TRAINED AND TESTED IN DIFFERENT DOMAINS. ALL THE RESULTS ARE EVALUATED IN THE TESTING SET.

	test in thin domain (thin CT image)				test in thick domain (thick CT image)			
Methods	AUC	ACC	SEN	SPE	AUC	ACC	SEN	SPE
$QuarterNet_{adaptive}$	0.883	0.831	0.805	0.861	0.881	0.838	0.849	0.824
$QuarterNet_{thin}$	0.875	0.828	0.836	0.818	0.670	0.588	0.398	0.818
$QuarterNet_{thick}$	0.775	0.690	0.938	0.390	0.888	0.821	0.894	0.733
$QuarterNet_{mix}$	0.845	0.770	0.907	0.604	0.858	0.831	0.727	0.916
$CyclGAN_{CT}$	0.645	0.496	0.137	0.930	0.600	0.547	1.0	0.00

Here, $f^{thin}(\cdot)$ and $f^{thick}(\cdot)$ represent the features extracted from the thin-CT branch and thick-CT branch, respectively. X^i_{thinCT} represent the thin-CT image and the thick-CT image of the $i-th$ patient.

For each branch in the Siamese-net, we employ a weighted binary cross-entropy loss. For the b_{th} branch network E^b, the loss function is:

$$L_{E^b} = -\sum_i \left(\left\{y^i = 0\right\} log_{10}\left(1 - E^b\left(X^i\right)\right) \cdot w_n + \left\{y^i = 1\right\} log_{10}\left(E^b\left(X^i\right)\right) \cdot w_p\right) \quad (3)$$

where w_n, w_p represent the loss weights for negative samples and positive samples respectively. During model training, the final loss function is:

$$L = \sum_i \left(\lambda L_s + \sum_b^2 L_{E^b}\right) \quad (5)$$

where λ is the hyper-parameter to weigh the feature similarity loss.

C. Dataset and implementation details

We collected a large dataset including 1413 lung cancer patients with both EGFR gene sequencing and multiple CT image series of different slice thicknesses from the West China Hospital. We randomly select 1000 patients as the training set, including 524 EGFR-mutant patients and 476 EGFR-wild type patients. The other 413 patients are used as the testing set, including 226 EGFR-mutant patients and 187 EGFR-wild type patients. All the patients in this dataset have multiple CT image series with various slice thicknesses. We treat CT images of slice thickness ranging from 0.75mm to 2mm as thin CT images (thin thickness domain); and CT images of slice thickness ranging from 3mm to 6.5mm as thick CT images (thick thickness domain). For each patient, we select both the thin CT and thick CT to construct an image pair to train the Siamese network. Before images were fed to the model, data augmentations methods including slight rotation and translation were randomly applied.

During model training, we set the hyper-parameters w_n, w_p, λ as 0.6, 0.4, 0.2 respectively, and use stochastic gradient descent (SGD) optimizer with the learning rate of 0.005 to train the model. To compare our method with state-of-the-art methods, and prove the effectiveness of our proposed two modules (QuarterNet and domain adaption network), all the comparison experiments used the same training parameters.

III. RESULT

We use area under curve (AUC), accuracy (ACC), sensitivity (SEN), and specificity (SPE) as evaluation metrics. To evaluate the performance of our network in predicting EGFR gene mutation status, we trained the QuarterNet on homogeneous CT images (i.e., only include CT images of the same thickness). As shown in Fig. 2 and TABLE II, the QuarterNets trained on thin thickness domain ($QuarterNet_{thin}$) or thick domain ($QuarterNet_{thick}$) achieved results with AUC=0.875 and 0.888 in the testing set when tested in the same domain. Both these two models achieved superior performance than the model published in a recent study (AUC=0.81) [2], indicating that through the QuarterNet to learn both local and global whole-lung features can achieve better performance than the commonly used tumor-based method.

However, due to the distribution gap, the model trained in one domain failed when tested in another domain. The $sQuarterNet_{thin}$ is trained in the thin domain; the performance drops from AUC=0.875 to AUC=0.670 when tested in the thick domain. Similarly, when we testing the $QuarterNet_{thick}$ in the thin thickness domain, the performance decreases from AUC=0.880 to AUC= 0.775 (TABLE II). These results indicate that deep learning models are very sensitive to CT image thickness. The most intuitive way to improve the robustness of models is increasing the diversity of training data, such as mixing both thin CT and thick CT in the training set. Consequently, we mixed both thin CT images and thick CT images to train the QuarterNet ($QuarterNet_{mix}$). This model achieved AUC=0.845 and 0.858 in the thin domain and thick domain, which showed improvement than directly testing the $QuarterNet_{thin}$ and the $QuarterNet_{thick}$ in the other domains. However, the performance of the $QuarterNet_{mix}$ still drops when compared with the model trained and tested in the same domain. Furthermore, we built a $CycleGAN_{CT}$ [11] model to transfer images into images with different thicknesses. Although the transferred images are visually indistinguishable from the ground truth, they failed in EGFR mutation status prediction.

Through the proposed domain adaptive network, Our $QuarterNet_{adaptive}$ model achieved remarkable performance in all metrics when tested in both two domains. The AUC reaches 0.883 and 0.881 in thin and thick domains, which outperformed the $QuarterNet_{mix}$ model that is commonly used in many studies. These results demonstrate that through the domain adaption strategy and the feature

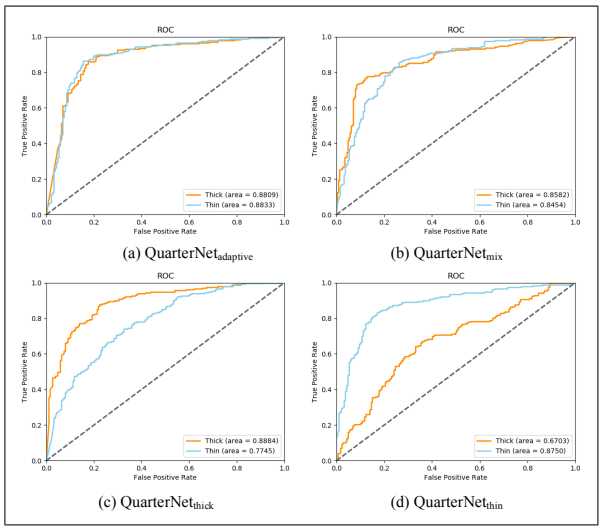

Fig. 2. ROC curves of the models. (a) the proposed $QuarterNet_{adaptive}$ model, (b) $QuarterNet_{mix}$ Model, (c) $QuarterNet_{thick}$ model, (d) $QuarterNet_{thin}$ model.

TABLE II

RESULTS OF THE MODELS WITH AND WITHOUT QUARTER-SPLIT STRATEGY.

Methods	test set	AUC	ACC	SEN	SPE
$QuarterNet_{adaptive}$	thin	0.883	0.831	0.805	0.861
	thick	0.881	0.838	0.849	0.824
$Non-quarterModel$	thin	0.866	0.806	0.894	0.701
	thick	0.875	0.741	0.584	0.930

similarity restriction in the two domains, the model successfully learned features that are invariant between different CT thicknesses.

In the QuarterNet, we used four networks to focus on learning local lung features from different lung lobes, and then mapped the local features into the whole lung for global lung feature learning. Through this local-global feature learning strategy, the $QuarterNet_{adaptive}$ model showed improvement compared with the model without the quarter-split network (Non-quarter split model) TABLE II in both thin and thick domains.

Compared with the previous study that only uses tumor area for analysis [2], our $QuarterNet_{adaptive}$ model is fully automatic without any manual tumor annotation and extracts more features from the whole lung. Through Grad-CAM visualization algorithm, we found that the $QuarterNet_{adaptive}$ model can automatically focus on peritumoral lung areas for analysis Fig. 3. This demonstrates that EGFR gene information can cause structural or anatomical changes in the whole lung instead of only inside tumor areas.

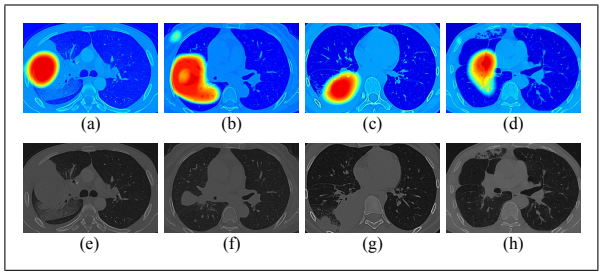

Fig. 3. The attention regions of the proposed $QuarterNet_{adaptive}$ model, which mainly focuses on lung regions around tumors. (a-d) are the attention heat maps and (e-h) are the corresponding CT images.

IV. CONCLUSIONS

In this paper, we present a novel fully automated $QuarterNet_{adaptive}$ model for non-invasive EGFR gene mutation prediction. This model used a quarter-split network to first learn local lung features and then learn global lung features, which showed a large improvement than commonly used tumor-based methods. Through the domain adaption strategy, the model learned thickness-invariant features that showed robust performance in CT images of different thicknesses. Furthermore, this study used a large dataset (1413 lung cancer patients) with EGFR gene sequencing and CT images of various thicknesses for a comprehensive evaluation. The results suggest that the $QuarterNet_{adaptive}$ model provides a robust tool for predicting EGFR mutation regarding heterogeneous CT images, which is important for individualized treatment planning in lung cancer.

REFERENCES

[1] National Comprehensive Cancer Network, "Non-Small Cell Lung Cancer," Apr. 2021. https://www.nccn.org/professionals/physician_gls/pdf/nscl.pdf.

[2] S. Wang et al., "Predicting EGFR mutation status in lung adenocarcinoma on computed tomography image using deep learning," Eur Respir J, vol. 53, no. 3, p. 1800986, Mar. 2019, doi: 10.1183/13993003.00986-2018.

[3] B. Houdu, "Why harmonization is needed when using FDG PET/CT as a prognosticator: demonstration with EARL-compliant SUV as an independent prognostic factor in lung cancer," Eur J Nucl Med Mol Imaging, p. 8, 2019.

[4] M. Meyer et al., "Reproducibility of CT Radiomic Features within the Same Patient: Influence of Radiation Dose and CT Reconstruction Settings," Radiology, vol. 293, no. 3, pp. 583–591, 2019.

[5] F. Orlhac, F. Frouin, C. Nioche, N. Ayache, and I. Buvat, "Validation of A Method to Compensate Multicenter Effects Affecting CT Radiomics," Radiology, vol. 291, no. 1, pp. 53–59, Apr. 2019, doi: 10.1148/radiol.2019182023.

[6] M. Shafiq-ul-Hassan, K. Latifi, G. Zhang, G. Ullah, R. Gillies, and E. Moros, "Voxel size and gray level normalization of CT radiomic features in lung cancer," Sci Rep, vol. 8, no. 1, p. 10545, Dec. 2018, doi: 10.1038/s41598-018-28895-9.

[7] J. Choe et al., "Deep Learning–based Image Conversion of CT Reconstruction Kernels Improves Radiomics Reproducibility for Pulmonary Nodules or Masses," Radiology, vol. 292, no. 2, pp. 365–373, Aug. 2019, doi: 10.1148/radiol.2019181960.

[8] Z. Alaverdyan, J. Jung, R. Bouet, and C. Lartizien, "Regularized siamese neural network for unsupervised outlier detection on brain multiparametric magnetic resonance imaging: Application to epilepsy lesion screening," Medical Image Analysis, vol. 60, p. 101618, Feb. 2020, doi: 10.1016/j.media.2019.101618.

[9] M. Dunnhofer et al., "Siam-U-Net: encoder-decoder siamese network for knee cartilage tracking in ultrasound images," Medical Image Analysis, vol. 60, p. 101631, Feb. 2020, doi: 10.1016/j.media.2019.101631.

[10] S. Wang et al., "A fully automatic deep learning system for COVID-19 diagnostic and prognostic analysis," Eur Respir J, vol. 56, no. 2, p. 2000775, Aug. 2020, doi: 10.1183/13993003.00775-2020.

[11] R. Oulbacha et al., "MRI to CT Synthesis of the Lumbar Spine from a Pseudo-3D Cycle GAN," in 2020 IEEE 17th International Symposium on Biomedical Imaging (ISBI), 2020, pp. 1784–1787.